# FATIGUE LIFE PREDICTION METHOD FOR COMPOSITE LAMINATE CONTAINING ARTIFICIAL FLAW USING ACOUSTIC EMISSION DETECTION

Batigne, C.[1]*, Maslouhi, A.[1], and Ganesan, R.[2]
[1] Département de Génie Mécanique, Université de Sherbrooke, Sherbrooke, Canada
[2] Department of mechanical, industrial and aerospace engineering, Concordia University, Montréal, Canada
* Corresponding author (Charly.Batigne@Usherbrooke.ca)

**Keywords***: Woven composites, Fatigue life prediction, Acoustic emissions*

## ABSTRACT

This paper presents a methodology to predict the fatigue life in a composite laminate containing an artificial embedded flaw, based on Acoustic Emission (AE) signals emitted by fatigue delamination onset in composite materials. To achieve this prediction, this model needs two main step analysis.

The first phase analysis is based on failure criterion obtained from experimental work on AE monitoring to detect the onset of delamination in plain weave carbon fiber coupons, that were prepared as per ASTM D5528 and D6671 standards. Delamination was characterized in quasi-static and fatigue testing, at different mixed-mode ratio values ($G_{II}/G_T$ = 0, 0.28, 0.37, 0.46, 0.75, 1) and at ambient temperature, high temperature and a set of combinations of temperature and humidity (22°C, 82°C dry, 82°C + 85% humidity). The collected AE signals have been processed to identify the onset of delamination and to establish a quasi-static failure criterion, using Double Cantilever Beam (DCB) and Mixed-Mode Bending (MMB) tests. Under fatigue loading, the coupons were tested at different energy release rate ratios (G*max*/Gc = 0.3 to 0.7) to generate a 3D fatigue failure criterion $G_{max}(G_{II}/G_T, N)$. As a comparison, Gc and G*max* have been calculated by the maximum load onset criterion in quasi-static tests and by the 5% compliance increase onset criterion in fatigue tests.

The second analysis calculates the Strain Energy Release Rate (SERR) variation around the flaw, by using finite element modeling of the laminate with the inserted flaw using Virtual Crack Closure Technique (VCCT) analysis, to identify where the delamination would most likely start propagating. Various external loads P were applied to evaluate the maximum value of the SERR and the corresponding mixed-mode ratio $G_{II}/G_T$. Then, an analytical function correlating $G_{II}/G_T$ and the SERR and a relation between the applied load P and the mixed-mode ratio is appointed and will be used in the prediction model.

For random values of applied load P, the value of mixed-mode ratio is calculated and then the corresponding fracture criterion estimated values from the 3D fatigue failure envelope. These correlations are then used to identify the number of cycles N corresponding to the SERR. The prediction curves of the load versus the fatigue life P(N) are then obtained. Experimental S-N curves have been generated previously for the same laminate, and they were compared with the predicted load versus the number of cycles curves.

## INTRODUCTION

Woven carbon fiber composites possess high mechanical properties in terms of strength to weight ratio and stiffness to weight ratio, excellent interlaminar shear properties and long fatigue life. These favorable properties have made them preferred materials for designing efficient, lightweight load-bearing structures. In the aerospace field, composite structures made of fabric usually operate under cyclic loading and may be exposed to high temperatures and moisture. These components can be manufactured by a variety of methods, and are joined by adhesive bonding, fastening or fusion bonding. Each manufacturing process may induce flaws such as voids, fiber misalignments, waviness, broken fibers and interfaces that have between layers delamination. Therefore, good engineering design requires a mechanics-based knowledge and damage evaluation based on the characterization of defects and quantification of their influence on mechanical performance characteristics and fatigue life. The prediction process for mechanical performance and durability has been well documented [1-3]. However, the development of a methodology to predict the fatigue life of the composite containing a flaw is still a challenge. Therefore, to develop an efficient prediction model, experimental data are needed to generate fatigue failure criterion. These results will then be combined with a finite element modeling and a Virtual Crack Closure Technique (VCCT) calculation in order to generate the fatigue life prediction model.

## EXPERIMENTAL FATIGUE FAILURE CRITERION

### Materials

The experimental testing is based on Acoustic Emission (AE) damage monitoring technique [4] to estimate the onset of delamination in plain weave carbon fiber coupons prepared following ASTM D5528 [5] and D6671 [6] standards. All tested samples were made of G30-500 PW Taffeta fabric carbon fiber pre-impregnated with CYCOM 5276-1 Epoxy, with a quasi-isotropic configuration $[45/0/-45/90]_{2S}$. The samples have a rectangular shape (150 x 25 mm) with a 3 mm thickness. The inserted flaw $a_0$ is 25 mm long. The coupons tested at high temperature and humidity have been conditioned in a controlled environment for 30 days, sealed and tested in a temperature-controlled chamber.

### Experimental procedures

All tests at ambient temperature were conducted on a MTS Test Frame 322 with a 5 kN load cell. All tests at specific temperature was conducted on a MTS Landmark 370 with a 2.5 kN 661.18F -02 load cell, in a MTS 651.06E-03 environmental chamber. Hinges were glued with an epoxy-based adhesive. The support span *2L* was fixed at 120 mm. A layer of nail polish was applied on the edges to evaluate the propagation of the delamination through a Dinolite camera x70. Test speed was fixed at 0.5 mm/s for quasi-static tests. For fatigue testing, all tests were conducted at 7 Hz under displacement control with a load ratio $G_{min}/G_{max}$ = 0.1 to avoid noise generation from friction. The test was stopped regularly at $\delta_{max}$ to measure the delamination length.

#### Acoustic emission parameters

Fatigue damage monitoring employing the acoustic emission technique was carried out using a piezoelectric sensor WD Rk02 from Physical Acoustics Corporation (PAC), glued to the surface of the laminate with a hot melt adhesive. A thin layer of high-vacuum grease was used as a coupling agent, and putty was applied to all hinges and surfaces that could induce noise. Table 2 presents the parameters used for AE monitoring.

Table 2: Acoustic Emission monitoring parameters

| **PAC WD Rk02** | | | |
|---|---|---|---|
| Broadband frequency | 100 kHz to 1 MHz | Amplification | 40 dB |
| Preamplifier | 2/4/6 | Sampling period | 500 ns |
| Acquisition threshold | 47 dB | Analysis | Noesis Software |

**Stress Energy Release Rate calculation**

Delamination was characterized in quasi-static and fatigue testing, at different mixed-mode ratio values ($G_{II}/G_T$ = 0, 0.28, 0.37, 0.46, 0.75, 1) and at ambient temperature, high temperature and high humidity (22°C, 82°C dry, 82°C + 85% humidity). The collected AE signals have been processed to identify the onset of delamination and to establish a quasi-static failure criterion $G_c(G_{II}/G_T)$, using Double Cantilever Beam (DCB) and Mixed-Mode Bending (MMB) tests. Under fatigue loading, the coupons were tested at different energy release rate ratios ($G_{max}/G_c$ = 0.3 to 0.7) to generate a 3D fatigue failure criterion $G_{max}(G_{II}/G_T, N)$. All the tests were conducted using the mechanical test bench presented on **Erreur ! Source du renvoi introuvable.**.

Figure 1: (a) Mixed-Mode Bending Test bench (b) Environmental chamber

The mode I SERR was calculated using the modified beam theory, as presented in the ASTM D5528 and considering the rotation of the two sides of the delamination during the test with the parameter $\Delta$ (equation 1). Mixed-mode SERR was calculated using equations 2 to 4 where only the mechanical properties were needed.

$$G_{Ic} = \frac{3P\delta}{2b(a+|\Delta|)} \tag{1}$$

$$G_I = \frac{3P^2(3c-L)^2}{4b^2h^3L^2E_{11}}\left[a^2 + \frac{2a}{\lambda} + \frac{1}{\lambda^2} + \frac{h^2E_{11}}{10G_{13}}\right] \tag{2}$$

$$G_{II} = \frac{9P^2(c+L)^2}{16b^2h^3L^2E_{11}}\left[a^2 + \frac{0.2h^2E_{11}}{G_{13}}\right] \tag{3}$$

$$\lambda = \sqrt[4]{\frac{3k}{bh^3E_{11}}} \qquad k = \frac{2bE_{22}}{h} \tag{4}$$

**Delamination onset threshold**

The various AE features extracted from waveforms were studied to assess the onset of delamination under fatigue loading. In the time domain, the distribution curves of amplitude, energy, and the number of counts versus the time of detected acoustic emission signals were studied to understand the delamination evolution function. The power spectrum was processed from AE signals in the frequency domain to assess the frequency features associated with different types of damage. The applied signal processing method lets picking thresholds of delamination onset. In fact, the threshold values were identified as the first observed peaks in the selected parameter distribution curve. An example of the damage threshold determination is shown in Figure 2.

Experimental tests were conducted at 1Hz with a non-filter on, to determine with precision the number of cycles corresponding to the delamination onset.

As described by Silversides [4] at lower stress states, most of the AE signals were generated by friction or fretting and not by damage initiation or growth. Early works have shown that material damage and friction both release energy and that emissions produced by the formation of new material surfaces release more energy than does the fretting of existing fracture surfaces. Therefore, friction and fretting emissions are characterized by low-level event intensities and occur throughout the entire range of cyclic stresses. AE discrimination of noisy AE was performed using a cluster analysis algorithm in Noesis software to identify loud signals associated with the frequent rubbing between existing fracture faces. Similar signals were then ranked and eliminated because non-relevant to delamination propagation. This procedure allowed us to determine delamination initiation more accurately. Thus, the first Peak observed in the selected feature distribution curve was defined as an initiation criterion. The corresponding time was used to determine the fatigue life of delamination onset.

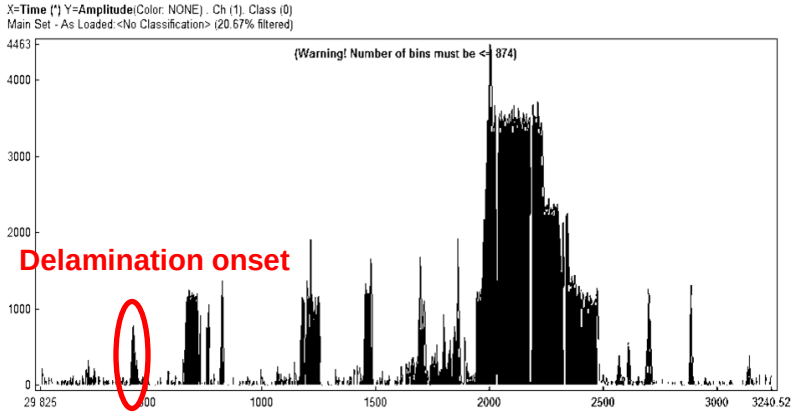


Figure 2 : AE amplitude distribution versus time for a mixed-mode GII/GT = 0,5 test and delamination onset threshold determination

**Fatigue failure criterion**

All fatigue tests were conducted at 7 Hz cycling frequency and under a displacement control with a load ratio $G_{min}/G_{max}$ = 0.1. Before characterizing the fatigue behavior under mixed-mode testing, specimens were tested under static loading to determine the extreme displacements, respectively δmax and δmin. The displacement control was chosen to allow a stable delamination propagation and avoid significant changes in the crack length. At specific cycles, mechanical tests were stopped to measure the delamination length with a Dynolite camera x70. AE distribution feature data allowed monitoring delamination onset value. This value was compared with the value corresponding to a 5% increase in compliance obtained by using the ASTM method [5].

Each sample was loaded at a $G_{max}$ value corresponding to a prescribed percentage of the quasi-static critical energy $G_c$. The $G_{max}$ values oscillated between 30% and 70% of Gc for each pure mode and mixed-mode ratios. Tests were conducted until a major crack was observed on the edges of the samples. Then the number of cycles before damage onset, obtained from AE emission signals, was associated with the $G_{max}$ value used for mechanical testing . A total of 8 trials were conducted to generate an entire G-N curve for each mixed-mode ratio, resulting in 40 tests for one environmental condition. Figure 3 presents an example of G-N curves generated for the dry condition of 22 °C dry. All results are normalized. The scales of the figure axis are normalized.

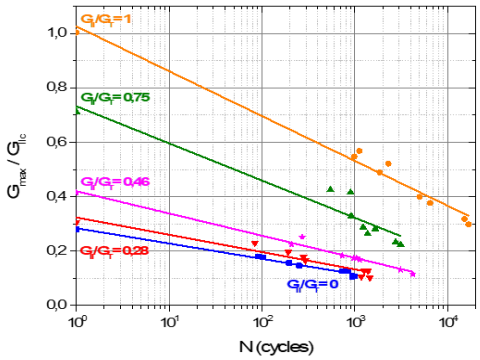


Figure 3 : G(N) curves generated from AE onset criterion under 22 °C dry condition

In fatigue failure prediction methodology, it is essential to determine the G-N curve for all mixed-mode ratios from 0 to 1. Thus, a delamination onset surface was generated from the two-dimensional G-N curves. The equation of this surface was extracted from the quasi-static failure criterion envelope, and the distinct G-N curves were obtained using equations 5 and 6. The parameters *a*, *b* and *c* are defined from the fitting surface on all fatigue results.

$$G_{max}\left(\frac{G_{II}}{G_T}, N\right) = G_c\left(\frac{G_{II}}{G_T}\right) - Blog(N) \tag{5}$$

$$B = a + b\left(\frac{G_{II}}{G_T}\right) + c\left(\frac{G_{II}}{G_T}\right)^2 \tag{6}$$

Three surfaces were generated that way, one for each environmental condition, with 40 tests per surface. An example of the surfaces generated is presented in Figure 4. The obtained analytical equations of these surfaces were then used in the fatigue failure prediction model.

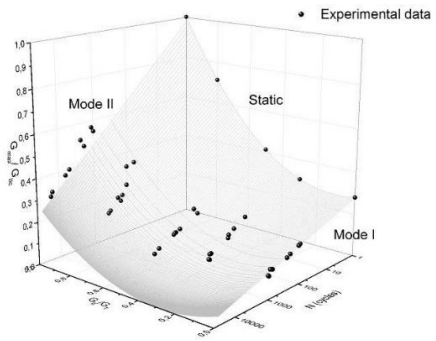


Figure 4 : Delamination onset surface obtained by using AE technique detection under pure mode and mixed-mode loadings at 22°C

**FINITE ELEMENT ANALYSIS AND APPLICATION of VCCT**

The finite element modeling of the laminate with inserted flaw using VCCT was conducted using ANSYS to determine the variation of Strain Energy Release Rate (SERR) around the flaw and to identify where the delamination is most likely to start propagating. The embedded flaw was modelled as free space. Layered solid elements SOLID 186 was used for VCCT analysis, and contact elements CONTAC 174 were used to bypass interpenetration of the different elements. Some CZM elements with no thickness and no properties were applied to define the crack path for the VCCT algorithm. The crack path was appointed around the flaw, and divided into four separate paths for easy computation. Figure 5 illustrates the 3D representation of the structure.

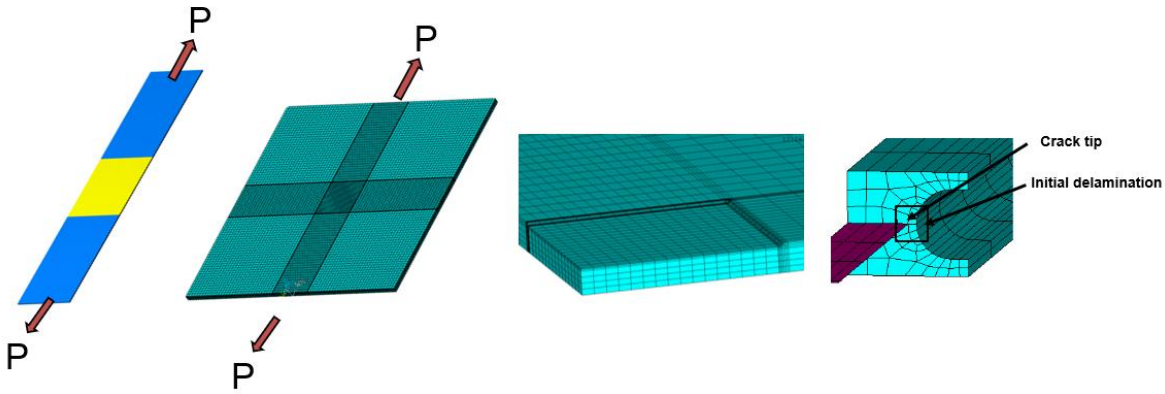


Figure 5 : Finite element representation of the sample, applied load and crack tip

The numerical model was validated by comparing the experimental load-displacement curve, and the one obtained using the finite element model. In addition, a comparison of the strain field was conducted between the one obtained from the numerical model and the strain variation measured by Digital Image Correlation (DIC) technique on the coupon.

Equations 7 to 9 help calculate the SERR values around the flaw by using the VCCT algorithm for a given load.

$$G_I = -\frac{1}{2\Delta a} Z_{Li}(w_{Ll} - w_{Ll*}) \tag{7}$$

$$G_{II} = -\frac{1}{2\Delta a} W_{Li}(u_{Ll} - u_{Ll*}) \tag{8}$$

$$G_{III} = -\frac{1}{2\Delta a} Y_{Li}(v_{Ll} - v) \tag{9}$$

A modified Benzeggagh-Kenane fracture criterion [7] was applied, as given by equation 10, to assess the onset of delamination from the flaw. As the load is increased, the algorithm performs calculations using this criterion around the flaw where the crack path is defined. When the criterion is met at the crack path, elements at the crack tip are separated, and the algorithm keeps calculating until the criterion is met again at the new crack tip. This procedure was repeated until the maximum load was reached.

$$f = \frac{G_I + G_{II} + G_{III}}{G_{Ic} + \frac{G_{II}(G_{IIc} - G_{Ic}) + G_{III}(G_{IIIc} - G_{Ic})}{G_I + G_{II} + G_{III}} \left[\frac{G_{II} + G_{III}}{G_I + G_{II} + G_{III}}\right]^{\eta - 1}} \tag{10}$$

This process was repeated for different load values, resulting in the establishment of two important relations needed for the fatigue life prediction model, as shown in Figure 7.

Firstly, a relation between the external applied load *P* and the total energy release rate $G_T$ was formed, as displayed in Figure 6 (a). Figure 6 (b) shows the second relationship, coupling the external applied load *P* and the mixed-mode ratio *GII/GT*. Equations 11 and 12 present these relations. The effect of temperature and humidity has not been considered in the numerical modelling.

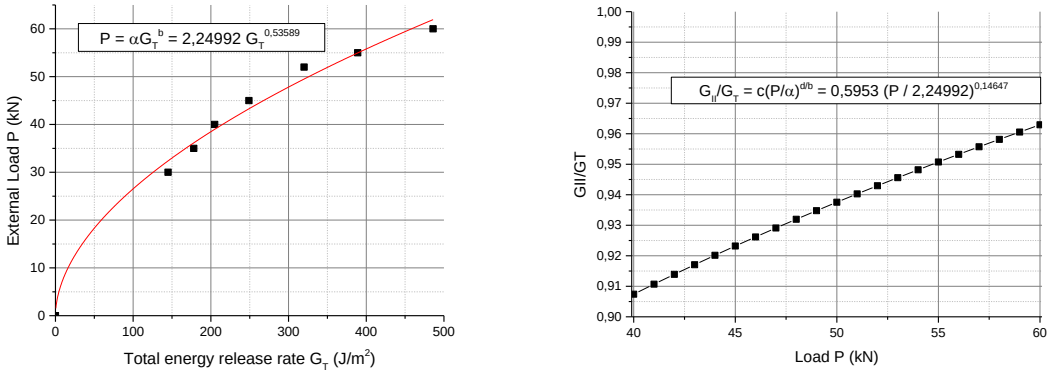


Figure 6 : Relation between (a) the externally applied load and the total SERR, (b) externally applied load and the mixed-mode ratio

$$P = 2.24992\ G_T^{0.53589} \tag{11}$$

$$\frac{G_{II}}{G_T} = 0.5953\left(\frac{P}{2.24992}\right)^{0.14647} \tag{12}$$

**FATIGUE LIFE PREDICTION MODEL**

The fatigue life prediction model is based on the fatigue failure criterion obtained from experimental testing and the two relations obtained with VCCT algorithm [8]. The finite element analysis calculated the total SERR and the mixed-mode ratio for an arbitrary value of applied load P. From this mixed-mode ratio, the corresponding curve $G_T(N)$ was extracted from the 3D experimental failure criterion, then the number of cycles at onset $N$ was determined. This process was repeated for different $P$ values, resulting in a full $P(N)$ curve. The full methodology is presented in Figure 7.

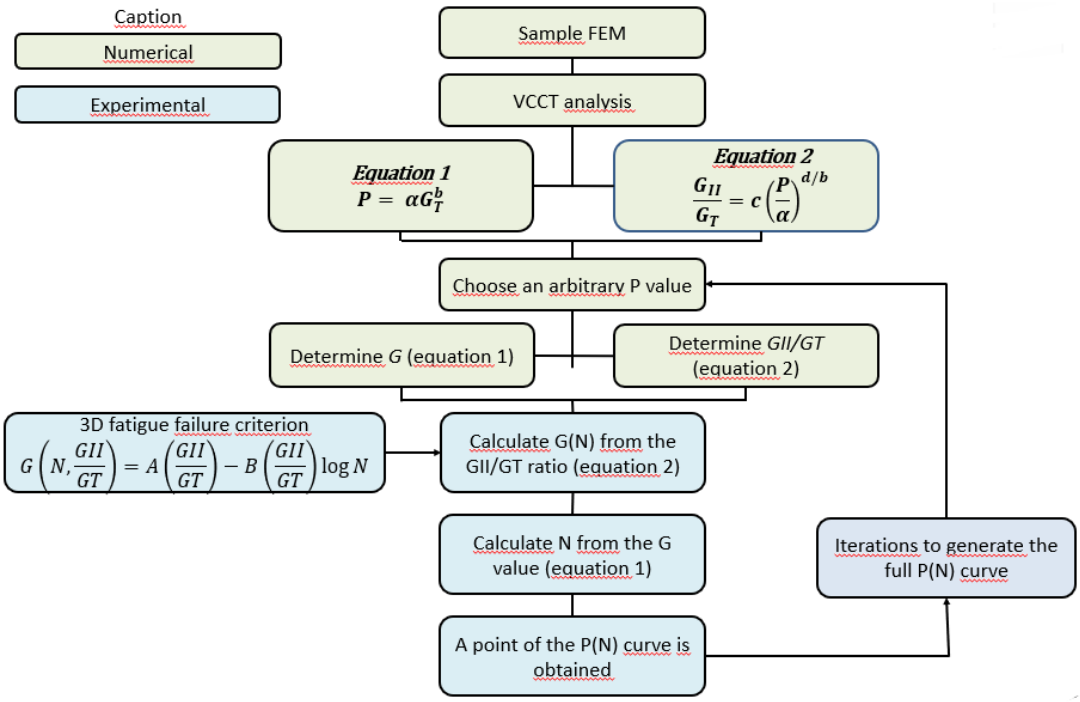


Figure 7 : Fatigue life prediction methodology

Experimental S-N curves have been generated previously for the same laminate and compared with the predicted ones. Figure 8 presents an example of the results of these predictions. The red curve corresponds to the experimental S-N curve generated using the AE technique to detect delamination initiation in coupons with the embedded flaw. The black curve was extracted from the same tests as the red curve. For these S-N curves, the failure criterion was defined at a specific reached strain value by our team collaborator from ETS (École de Technologie Superieure) [9]. The proposed criterion considers that delamination occurs when the laminate reaches a total deformation of 5%. This approach was supported by microscopic observations of the laminate post-test [9]. The blue curve represents the predicted S-N curve generated by the developed model.

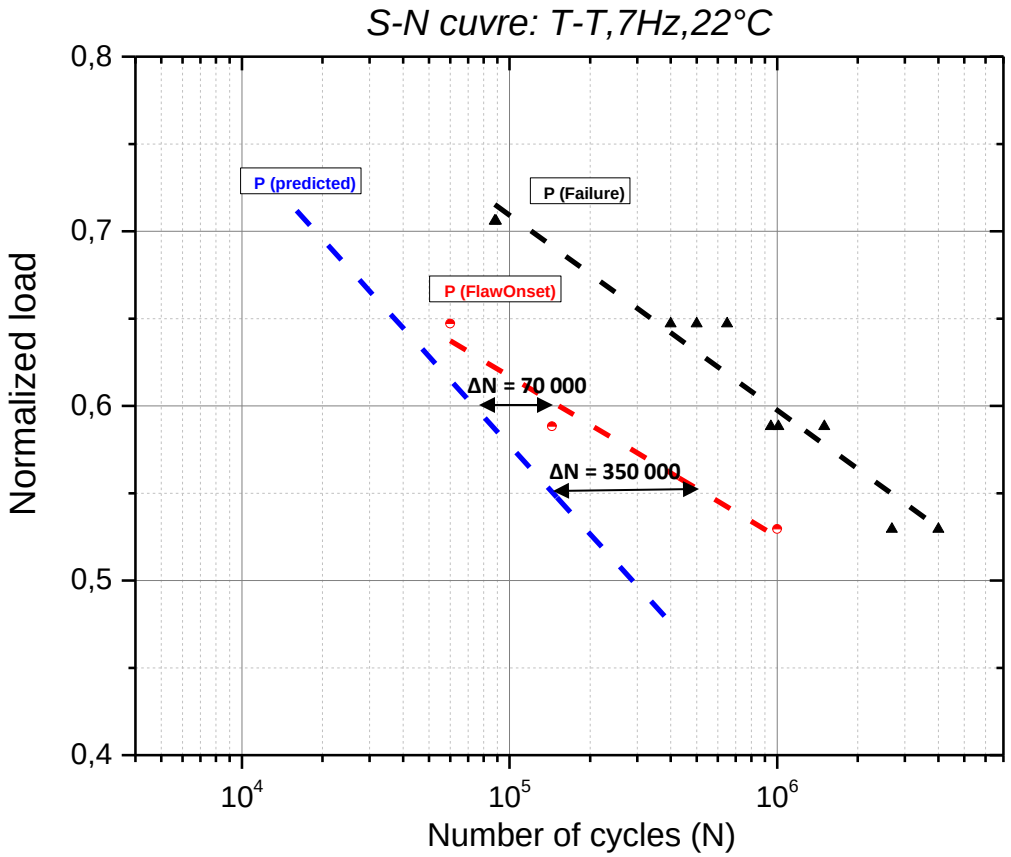


Figure 8: Experimental and predicted S-N curves under fatigue tension-tension loading at 7 Hz and 22°C

The prediction reveals a good correlation with the experimental S-N curve. For a given external load *P*, the prediction model provides a corresponding number of cycles *N* slightly lower than the one obtained from the experimental results. The average difference between the prediction and experimental results is around 30 %.

However, the finite element model does not perfectly represent the inserted artificial defect in experimentally tested composite samples. We assume the presence of imprecision due to the inserted folded Teflon tape's curvature. Furthermore, imprecision due to the shape extremities of the defect and disregard for the composite woven configuration in the numerical model. This being said, we consider the prediction results acceptable and permit an allowable safety margin in fatigue life to avoid excessive delamination propagation in the structure.

The main advantage of this method is the possibility of assessing another structure's fatigue life, as long as the same material is used. The only step needed is numerical modelling of the structure to achieve that, and then the application of the VCCT algorithm will help to calculate the strain energy release rate values and to conclude on delamination appearance, as presented in this article.

## CONCLUSION

This article presented the development of a methodology to predict the onset of delamination under fatigue loading in laminated samples comprising an embedded flaw. The procedure is based on determining experimental fatigue failure criterion by employing ASTM standards delamination tests in mode I, mode II, and mixed-mode I and II. Also, on the generation of two analytical functions, $P(G_T)$, $P(G_{II}/G_T)$, coupling load and strain energy release rate values were obtained via finite element modelling and VCCT analysis. The obtained prediction model was then compared with the fatigue life curves generated by experimental testing, and it showed an acceptable correlation. The effect of temperature and humidity has only been considered in the experimental part of the prediction model and not in the numerical modelling.

## ACKNOLEDGEMENTS

This study was supported by the Natural Sciences and Engineering Research Council of Canada (NSERC), the Consortium for Research and Innovation in Aerospace in Quebec (CRIAQ) and the Centre de recherche sur les systèmes polymères et composites à haute performance (CREPEQ).

## REFERENCES

[1] M. Ratwani. "*Effect of damage on strength and durability*", NATO Research and Technology Organization. 2010.

[2] R. Talreja and C. Veer Singh. "*Damage and failure of composite materials*", Cambridge university press. 2012.

[3] R.H. Martin. "Incorporating interlaminar fracture mechanics into design", *Proceedings of The Institution of Mechanical Engineers Part L-journal of Materials-design and Applications - PROC INST MECH ENG L-J MATER*, 214, pp. 91-97. 10.1243/1464420001544870. 1998.

[4] I. Silversides, A. Maslouhi and G. Laplante. "Acoustic Emission Monitoring of Interlaminar Delamination Onset in Carbon Fibre Composites", *Structural Health Monitoring*, 12(2), pp. 126-140. 2013

[5] ASTM D5528. "Standard test method for mode I interlaminar fracture toughness of unidirectional fiber-reinforced polymer matrix composites", *ASTM International. 2013*

[6] ASTM D6671. "Standard test method for mixed mode I – mode II interlaminar fracture toughness of unidirectional fiber reinforced polymer matrix composites", *ASTM International*. 2010

[7] Bui Q.V. "A modified Benzeggagh-Kenane fracture criterion for mixed-mode delamination", *Journal of Composite Materials*, 45(4), pp. 389-413. 2011

[8] Composite Materials Handbook. *"Polymer matrix composites : materials usage, design and analysis"*. SAE Internationl, pp 12-91 – 12-97. 2012.

[9] Wu.J. "*Étude du comportement en fatigue des composites tissés et détermination des seuils d'initiation des endommagements*", Master thesis, 2016.